



# Grain size measurement using a semi-automatic calculation tool

Fatah Mernache\* , Abdelaziz Sehisseh , Amina Amrane , Said Hadji ,  
Yasmine Melhani , Mohamed Grine , Lakhdar Messai 

Fuel Department, Nuclear Research Center of Draria, B.P. 43 Sebala, Draria, Algiers, Algeria.

## Abstract

This paper focuses on the development of a semi-automatic calculation tool to measure the Mean Linear Intercept (MLI) grain size of ceramics and other materials.

The calculation tool was first verified and validated by using a certified micro-ruler and literature microstructures. It was then used to investigate the grain growth of  $\text{UO}_2$  pellets elaborated under different conditions. The tool offers the advantage of accuracy as well as the ability to quantify microstructures obtained with poor image quality. The estimated measurement errors were found to be less than  $1 \mu\text{m}$ .

The developed tool, mainly for the purpose of time-saving, allowed us to follow the microstructure (grain size) evolution of the elaborated  $\text{UO}_2$  fuel with different additives.

**Keywords:** image analysis, grain size, calculator tool, microstructure

## 1. Introduction

Grain size is the most commonly performed microstructural measurement, whether for quality control or research purposes (Vander-Voort, 1993). Its determination with accuracy requires high-quality images using optical microscopy.

The grain size of  $\text{UO}_2$  is an important parameter in the performance of reactor fuel elements (White, 1997). After the Fukushima accident in 2011, accident tolerant fuels (ATF) attracted considerable attention from researchers. One of the ATF fuel types, large grain  $\text{UO}_2$  fuel is characterized by the greatly increased  $\text{UO}_2$  grain size, achieved with certain additives (Zhong et al.,

2021). Thereby, it can reach higher burn-up than normal  $\text{UO}_2$  fuel (Hastings, 1983; Milena-Pérez et al., 2021; Turnbull, 1974; Une et al., 1993). Many authors have investigated the effect of process parameters on the grain growth of  $\text{UO}_2$  pellets, which mainly include chemical additives (dopants) and recycled material ( $\text{U}_3\text{O}_8$ ) (Bourgeois et al., 2001; Song et al., 2000; Yang et al., 2012).

Measurement of grain growth can be done by any of the microscopy techniques described by some standards (ASTM E112, 2013; ASTM E1382, 2015). ASTM E112 describes the linear intercept method in general and the Heyn procedure (Heyn, 1903) in particular to measure grain size by image analysis. However, this method is manual and does not describe any automated procedure for grain size measuring.

\* Corresponding author: [f-mernache@crnd.dz](mailto:f-mernache@crnd.dz)

ORCID ID's: 0000-0002-8089-9081 (F. Mernache), 0000-0003-4529-2556 (A. Sehisseh), 0000-0001-8526-7588 (A. Amrane), 0000-0001-7712-0666 (S. Hadji), 0000-0002-4639-7459 (Y. Melhani), 0000-0001-7457-3619 (M. Grine), 0000-0002-9657-5006 (L. Messai).  
© 2023 Authors. This is an open access publication, which can be used, distributed and reproduced in any medium according to the Creative Commons CC-BY 4.0 License requiring that the original work has been properly cited.

In recent years, image analyzers for grain size measurement have become much more powerful, faster, and fully automated. However, when automatic image analyzers are employed, poor microstructure quality leads to measurement errors.

Automatic image analysis methods are based on statistical estimations. They could provide the correct result if all the grain boundaries are revealed yet this is never the case.

The mean grain size of a ceramic is almost always determined either manually or semi-automatically, using too few grains (Arnould et al., 2001). The revealing of ceramic oxide microstructures is generally difficult. For example, the chemical etching of uranium dioxide (UO<sub>2</sub>) is difficult to control and reproduce, and revealing grain boundaries is often incomplete. Moreover, inclusions and other similar constituents within grains may be detected as grain boundaries. For all these reasons, a semi-automatic tool to determine the grain size is needed. The study aims to verify and validate the developed semi-automatic calculator tool. This tool is then used to investigate the grain size measurements for UO<sub>2</sub> pellets elaborated under different conditions.

## 2. Material and methods

The grain size measurements of multiple images at different magnification scales (literature and elaborated microstructures) were performed using the developed tool. This tool was first calibrated using a Zeiss certified ruler (Zeiss, 1 mm).

### 2.1. Sample preparation

Metallographic sample preparation must be controlled to produce acceptable quality surfaces for microstructure analysis using the calculation tool. This can be done by following standards such as the American Society for Testing and Materials (ASTM E3 or C1868).

### 2.2. Grain size calculation

The mean linear intercept (MLI) method is a common, widely used way to calculate averaged grain sizes (Abrams, 1971; Higginson & Sellar, 2003; Koskenniska et al., 2020). It is described in detail in the ASTM E112 standard (ASTM E112, 2013). In this method, horizontal and/or vertical lines are drawn on the microstructure images, and the number of times each line segment intersects a grain boundary is counted. An intersection is

a point (1) where a test line crosses a grain boundary. Segments at the end of a test line, which penetrate into a grain, are scored as half intercepts (1/2). A tangential intersection with a grain boundary should be scored as one intersection (1). An intersection coinciding with the junction of three grains should be noted as 1 & 1/2.

The average size is given by using Equations (1) and (2) (Abrams, 1971; Higginson & Sellar, 2003; Koskenniska et al., 2020).

$$\bar{L} = \frac{\sum L}{\sum x} \quad (1)$$

where:  $\bar{L}$  – MLI;  $\sum L$  – actual size of measurement lines;  $\sum x$  – measurement line interceptions with the grain boundaries.

Image magnification is used to convert measurement lines into actual size as shown by Equation (2).

$$\frac{L}{L_{im}} = \frac{L_g}{L_{g,im}} \rightarrow L = \frac{L_g}{L_{g,im}} L_{im} \quad (2)$$

where:  $L_{im}$  – length of measure line in an image;  $L_g$  – actual size length of a gauge line;  $L_{g,im}$  – length of a gauge line in an image.

In case of biphasic material, the MLI should be expressed (ASTM E1382, 2015) by multiplying the Expression (1) by the area fraction  $\bar{A}_A$  relating to the phase of interest:

$$\bar{L}_A = \frac{\sum L}{\sum x} \cdot \bar{A}_A \quad (3)$$

Statistical errors in grain size measurement were calculated as the mean standard deviation.

### 2.3. Calculator tool

Manual methods for grain size measurement are described in detail in the ASTM E112 standard. Those methods are time-consuming and less efficient because of possible human errors. Furthermore, as the required precision is high, there is a great need for its automation.

A novel calculator tool written using visual Pascal language has been developed to measure the MLI grain size of materials. Its principle is to calculate the number of intercepts at the intersection of a test line of known length with the grain interface, and use the intercept per unit length to determine the MLI grain size. The magnification is chosen so that at least 100 grains are within the test area. At the end of the measurements, the MLI grain size is calculated by dividing the total length of measure lines by the amount of grain boundary intercepts. The

calculator tool include an algorithm that was established to measure the MLI grain size for each test line. As can be seen in Figure 1, its interface is presented in the form of windows inviting the operator to sequentially:

- load the micrograph image to be characterized (Fig. 1a);
- define the used measurement calibration factor or the used magnification (Fig. 1b);
- choose the appropriate zoom, which allows displaying of enough grains to draw a test line;
- trace a test line using two consecutive clicks on the image (Fig. 1c);

- click suitably on each intercept to define its nature (single intercept, tangent, end or triple). The operator uses the left and right mouse buttons combined with the Ctrl or shift keys on the keyboard to define the nature of the intercept (Fig. 1d). The user is invited to redo the estimate MLI on another field; otherwise, the measurements are finished and the developed tool calculates the MLI grain size of all the fields processed (Fig. 1e). In the case of a material having more than one phase, the fraction of the phase of interest is taken into account in the MLI calculations.

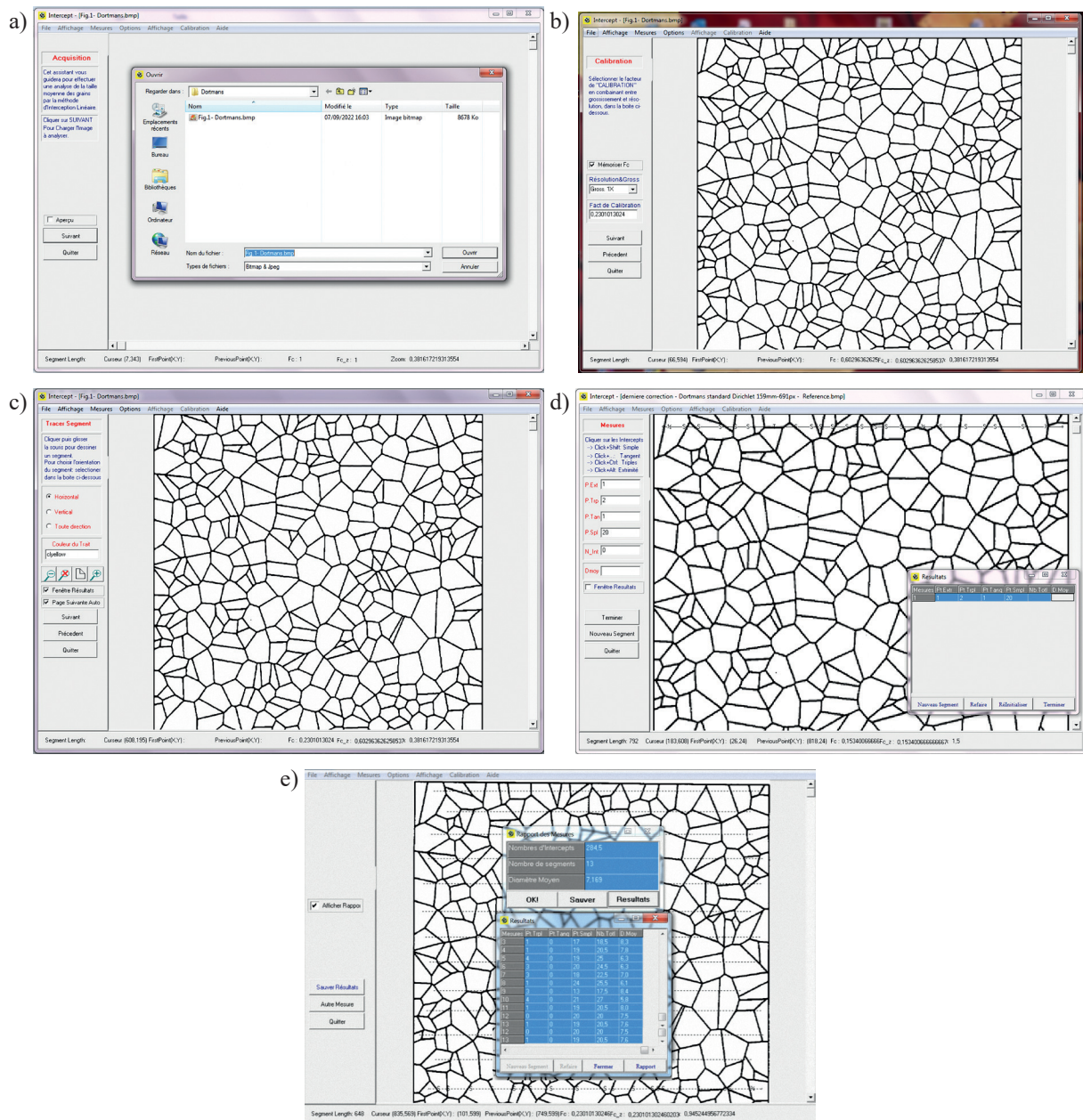


**Fig. 1.** Illustration of sequential steps of MLI measurements by calculator tool: a) image acquiring; b) calibration factor setting; c) preparing and tracing of a segment; d) intercept processing for the traced segment (nature of intercepts); e) summary report of MLI results

### 3. Results

In this work, the developed procedure principle is to measure grain size semi-automatically by drawing a line on every grain using the calculator tool. Grain size quantification of literature and elaborated  $\text{UO}_2$  microstructures were done using the developed tool as described above.

#### 3.1. Verification and validation of the calculator tool

Before using the developed calculator tool to study the additions effect on elaborated  $\text{UO}_2$  pellets microstructures, we have to verify that it meets the requirements for the specified application. For this purpose, the tool was first tested using a certified Zeiss graduated ruler and then literature micrographs. A computer drawn microstructure from the literature (Dortmans et al., 1993; Fig. 1) was used for grain size quantification. This microstructure was generated as a pseudo-random two-dimensional Dirichlet tessellation and contained 350 grains with non-porosity. On the original image, 159 mm is equal to 691 pixels, thus the calibration factor calculated is 0.23 mm/pixel.

For the repeatability of the grain size measurements using the calculator tool, five tests were carried out with the computer drawn microstructure. The results are shown in Table 1.

**Table 1.** Computer drawn microstructure and measured grain sizes by the calculator tool [mm]

Trials	1	2	3	4	5
Grain size	7.26	7.32	7.17	7.33	7.39
Mean grain size ( $\bar{L}$ )	7.29				
Standard deviation for $\bar{L}$	0.07				

An example (3<sup>rd</sup> test in Table 1) of the grain size measurement results obtained with the tool after the final processing step is presented in Figure 1e. The grain size was automatically calculated for each line. The result of the measurements was an arithmetic mean of the different grain sizes obtained.

As we can see in Figure 1e, the test lines number is 13, the number of intercepts at the intersection of a test line with the grain interface (grain boundary) is 284.5 and the MLI grain size is  $\sim 7.17$  mm.

The grain sizes results obtained by 04 different operators using the computer drawn microstructure are summarized in Table 2. The mean grain size

obtained is 7.29 mm with a standard deviation of 0.08 mm. Dortmans et al. (1993) reported the mean grain size result of measurements carried out by twenty-five participants from different countries. They found  $7.01 \text{ mm} \pm 0.41 \text{ mm}$ .

The amount of scatter, defined as “2 · standard deviation/mean value”, between the four operators is less than 2.5%. This scatter is probably due to the influence of the random positioning of lines on the micrograph and the misinterpretation of grain boundaries.

Some  $\text{UO}_2$  micrographs from previous literature (Ben Saada, 2017; Gonzaga et al., 2008; Song et al., 2000) were selected for grain size measurement using the calculator tool. The grain boundaries of some of these micrographs are not all fulfilled. Moreover, the interior of some grains is of different intensity value from the neighboring grains. This is mainly due to the etching process that is a manual skill based process. By using commercially available image analysis software, it is difficult to analyze these micrographs.

The measurement results obtained by four operators for the literature  $\text{UO}_2$  pellets micrographs are shown in Table 2. The means grain sizes measured after processing the two first  $\text{UO}_2$  micrographs (Ben Saada, 2017; Figs. 11a, b) are respectively  $4.65 \mu\text{m} \pm 0.88 \mu\text{m}$  (ref. Ben Saada, 2017; Fig. 11a; measurement:  $<10 \mu\text{m}$ ) and  $23.50 \mu\text{m} \pm 0.92 \mu\text{m}$  (ref. Ben Saada, 2017; Fig. 11b; measurement:  $>20 \mu\text{m}$ ). The results are in accordance with those obtained by micrographs author.

Observation of two other selected  $\text{UO}_2$  micrographs from the literature (Gonzaga et al., 2008; Song et al., 2000) indicates that the grain boundaries were better revealed. The interior of grains and the boundary separating the grains are of different intensity value. The mean grain sizes obtained using the calculator tool after processing the micrographs illustrated in works by Gonzaga et al. (2008; Fig. 6) and Song et al. (2000; Fig. 9) are  $9.73 \mu\text{m} \pm 0.95 \mu\text{m}$  and  $8.18 \mu\text{m} \pm 0.88 \mu\text{m}$  respectively. These values are close to those found by these authors respectively ( $9.6 \mu\text{m}$  – Gonzaga et al., 2008, and  $08 \mu\text{m}$  – Song et al., 2000; see Table 2).

#### 3.2. Elaboration of $\text{UO}_2$ pellets with additives

Three different uranium dioxide ( $\text{UO}_2$ ) fuels with various additions have been fabricated and characterized. 5 wt%  $\text{U}_3\text{O}_8$  and 0.2 wt%  $\text{Cr}_2\text{O}_3$  were added to pure  $\text{UO}_2$  powder, which was produced through the Ammonium Uranyl Carbonates (AUC) process. The O/U ratio of the pure  $\text{UO}_2$  powder is 2.11. The specific BET surface areas of the  $\text{UO}_2$  and  $\text{U}_3\text{O}_8$  powders are  $5.8 \text{ m}^2/\text{g}$  and  $0.8 \text{ m}^2/\text{g}$ , respectively.

**Table 2.** Grains sizes results obtained by 04 operators using literature  $\text{UO}_2$  pellets micrographs

Micrograph [ref.]	Mean grains size [ $\mu\text{m}$ ]					
	operator 1	operator 2	operator 3	operator 4	four operators	[ref.]
Dortmans et al., 1993; Fig. 1	7.17	7.39	7.31	7.31	$7.29 \pm 0.08$	$7.01 \pm 0.41$
Ben Saada, 2017; Fig. 11a	5.15	5.85	3.77	3.83	$4.65 \pm 0.88$	<10
Ben Saada, 2017; Fig. 11b	25.08	22.96	22.90	23.05	$23.50 \pm 0.92$	>20
Gonzaga et al., 2008; Fig. 6	8.89	9.28	11.34	9.40	$9.73 \pm 0.95$	9.6
Song et al., 2000; Fig. 9	7.36	8.47	9.50	7.38	$8.18 \pm 0.88$	08

$\text{UO}_2$  pellets without additives, the so-called standard pellets (Std), pellets containing as additive 5 wt%  $\text{U}_3\text{O}_8$  (oxidized uranium pellet scrap – OS) or 5 wt%  $\text{U}_3\text{O}_8 + 0.2$  wt%  $\text{Cr}_2\text{O}_3$  (oxidized uranium pellet scrap and chromium oxide – OSCO) were produced. The two batches OS and OSCO were prepared by mixing the  $\text{UO}_2$ ,  $\text{U}_3\text{O}_8$  and  $\text{Cr}_2\text{O}_3$  powders in the proper proportion in a Turbula mixer for 24 h. The green pellets were prepared by the conventional powder metallurgy technique. All samples were pressed into green pellets at 400 MPa. Sintering of the green pellets was done in a furnace at 1550°C and 1600°C for 3 h in reducing atmosphere (Ar–10%  $\text{H}_2$ ) with a 10°C/min heating rate.

The microstructure preparation of  $\text{UO}_2$  pellets was made in accordance with ASTM C1868 (ASTM C1868, 2018) relating to the ceramographic preparation of namely  $\text{UO}_2$  pellets for microstructural analysis. The sintered pellets were cut on an axial plan, polished and chemically attacked (9 : 1 mixture of  $\text{H}_2\text{O}_2$  with  $\text{H}_2\text{SO}_4$ ) to distinguish grain boundaries. The metallographic observations of  $\text{UO}_2$  samples and the photographs taken were made using an optical microscope (Zeiss) coupled to a high-resolution digital camera. The acquisition software used is Karl Zeiss AxioVision. The magnification calibration was performed with a certified graduated micro-ruler (Zeiss, 1 mm).

After pressing the powders prepared by the above process, the cylindrical green pellets obtained have a diameter and height of the order of 10 mm. Sintered pellets having about 7.8 mm in diameter and 8.4 cm in height were formed. The oxygen to uranium (O/U) ratio of the sintered pellets is between 2.01 and 2.02 ( $\pm 0.01$ ). Sintered densities determined by the Archimedes water immersion method are high (more than 95% TD – Theoretical Density). The porosity rate of  $\text{UO}_2$  pellets is therefore low.

### 3.3. Grain size measurement of the elaborated $\text{UO}_2$ pellets

The average grain size of elaborated  $\text{UO}_2$  pellets was first determined using the calculator tool. It was estimated with up to ten images per sample. At least 100 grains were analyzed for each pellet. The results are summarized in Table 3.

For comparison, other estimates of the  $\text{UO}_2$  pellets grain size (Table 3) were made by the planimetric method, according to standards ASTM E112 and E1382. The greatest difference between measurements using the two methods was 1.5  $\mu\text{m}$ . This is probably due to the misinterpretation of grain boundaries that are unclear in some microstructures.

**Table 3.** Grain size measurements of the elaborated  $\text{UO}_2$  pellets using the intercept method (calculator tool) and planimetric method

$\text{UO}_2$ pellets	Grain size [ $\mu\text{m}$ ]			
	1550°C		1600°C	
	calculator tool	planimetric method	calculator tool	planimetric method
Std	7	8.3	9	9.1
OS	8	9.5	11	9.9
OSCO	10	9.8	16	16.0

At 1550°C (Fig. 2) grain size increased slightly (Std pellet: 7  $\mu\text{m}$ ; OS pellet: 8  $\mu\text{m}$ ; OSCO pellet: 10  $\mu\text{m}$ ). However, a significant increase in grain size is obtained for OSCO pellets sintered at 1600°C (Fig. 3, 16  $\mu\text{m}$ ). This confirms that the  $\text{Cr}_2\text{O}_3$  increased the grain size of  $\text{UO}_2$  fuel.

As expected, larger grains are obtained for higher sintering temperature and  $\text{Cr}_2\text{O}_3$  doped pellet.  $\text{Cr}_2\text{O}_3$  addition to  $\text{UO}_2$  fuel increases the densification rate and greatly increase the average grain size.

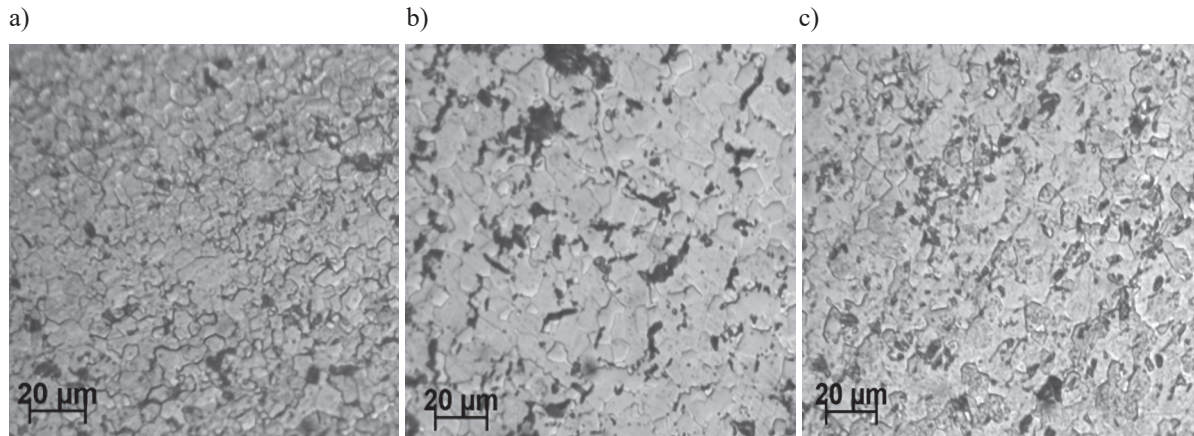


**Fig. 2.** Microstructures of sintered  $\text{UO}_2$  compacts at  $1550^\circ\text{C}$  and elaborated in different conditions  
a) Std pellet; b) OS pellet; c) OSCO pellet

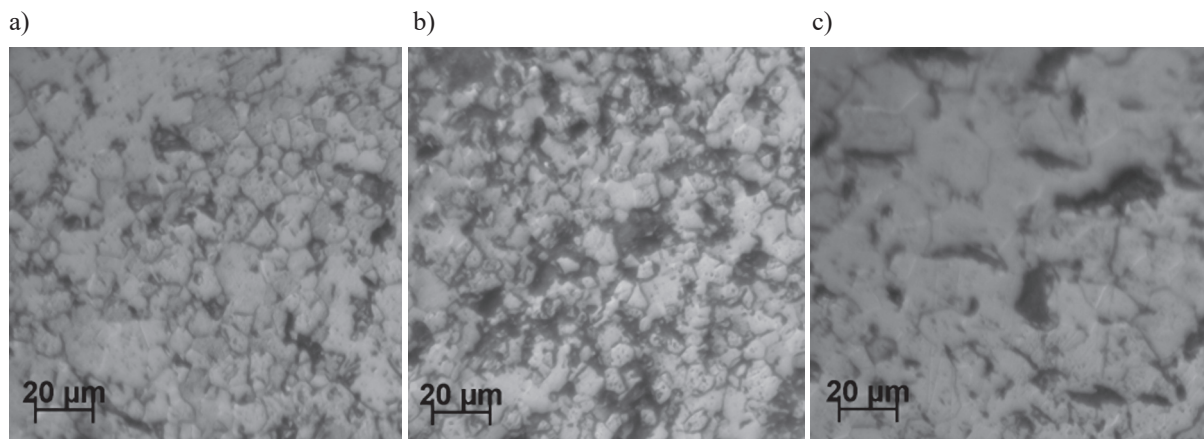


**Fig. 3.** Microstructures of sintered  $\text{UO}_2$  compacts at  $1600^\circ\text{C}$  and elaborated in different conditions:  
a) Std pellet; b) OS pellet; c) OSCO pellet

Grain boundary energy delivers the driving force for grain growth. In a pure  $\text{UO}_2$  system (Bourgeois et al., 2001), the grain growth is determined by grain boundary diffusion.  $\text{Cr}_2\text{O}_3$  addition until the solubility limit of  $\text{Cr}_3^+$  in  $\text{UO}_2$  is reached (Milena-Pérez et al., 2021) leads to larger  $\text{UO}_2$  grains because of enhanced grain boundary mobility.

#### 4. Conclusion

In this paper, a semi-automatic grain size calculator tool was developed and tested with known images. It is based on a line intercept procedure of ASTM E112-13 standard and the operator takes part in decision-making. Some microstructures from the literature were quantified for comparison, and the uncertainties of the results were evaluated. After that, the grain sizes of elaborated  $\text{UO}_2$  pellets with additives ( $\text{U}_3\text{O}_8$  and  $\text{Cr}_2\text{O}_3$ ) were measured using the calculator tool.

With commercial softwares, poor quality images introduce significant uncertainties in the evaluation of microstructural properties of the  $\text{UO}_2$  pellets due to the computational methodologies used to estimate the average grain size.

Grain size measurement with the calculator tool was satisfactory regarding the presented results. It permitted better results to be obtained than by the manual or automatized method. A large number of grains can be analyzed, which brings a greater statistical representation to grain size measurement. In addition, the analysis of the microstructures stored in the computer can be quickly repeated and a degree of precision can be obtained in a short time.

From the discussed results, the measurement errors (operator errors) were estimated to be less than  $1 \mu\text{m}$ . The amount of scatter between the operators is probably due to the interpretation of the microstructure and the influence of random positioning of lines on the micrographs.

The use of the tool has allowed us to understand the effects of additives ( $\text{Cr}_2\text{O}_3$  and  $\text{U}_3\text{O}_8$ ) on the  $\text{UO}_2$  fuel microstructural (grain size) evolution. Currently, several engineers and researchers at the Nuclear Research Center of Draria, Algiers, Algeria, are using the developed grain size calculator.

## Acknowledgements

The authors would like to thank Prof. Mahmoud Izerrouken and Dr. Nabil Kherrouba for their comments and suggestions.

## References

- Abrams, H. (1971). Grain size measurement by the intercept method. *Metallography*, 4(1), 59–78. [https://doi.org/10.1016/0026-0800\(71\)90005-X](https://doi.org/10.1016/0026-0800(71)90005-X).
- Arnould, X., Coster, M., Chermant, J.L., Chermant, L., Chartier, T., & Elmoataz, A. (2001). Segmentation and grain size of ceramics. *Image Analysis & Stereology*, 20(3), 131–135. <https://doi.org/10.5566/ias.v20.p131-135>.
- ASTM C1868-18 (2018). *Standard Practice for Ceramographic Preparation of  $\text{UO}_2$  and Mixed Oxide (U,Pu) $\text{O}_2$  Pellets for Microstructural Analysis*.
- ASTM E112-13 (2013). *Standard Test Methods for Determining Average Grain Size*.
- ASTM E1382-97 (2015). *Standard Test Methods for Determining Average Grain Size Using Semi-automatic and Automatic Image Analysis*.
- ASTM E3-11 (2017). *Standard Guide for Preparation of Metallographic Specimens*.
- Ben Saada, M. (2017). *Étude du comportement visco-plastique du dioxyde d'uranium. Quantification par analyse EBSD et ECCI des effets liés aux conditions de sollicitation et à la microstructure initiale* [Ph.D. Thesis, University of Lorraine]. <http://www.theses.fr/2017LORR0270>.
- Bourgeois, L., Dehaut, P., Lemaignan, C., & Hammou, A. (2001). Factors governing microstructure development of  $\text{Cr}_2\text{O}_3$ -doped  $\text{UO}_2$  during sintering. *Journal of Nuclear Materials*, 297(3), 313–326. [https://doi.org/10.1016/S0022-3115\(01\)00626-2](https://doi.org/10.1016/S0022-3115(01)00626-2).
- Dortmans, L.J.M.G., Morrell, R., & With, G., de (1993). Round robin on grain size measurement for advanced technical ceramics. *Journal of the European Ceramic Society*, 12(3), 205–213. [https://doi.org/10.1016/0955-2219\(93\)90122-8](https://doi.org/10.1016/0955-2219(93)90122-8).
- Gonzaga, R., Da Silva Gonçalves, J., Matos, C.A., de, & Souza Motta, E., de (2008). *Study of the microstructural variations (average grain size) on  $\text{UO}_2$  pellets in relation to the Si and Al contents, in production scale*. Research Gate. [https://www.researchgate.net/publication/237612197\\_Study\\_of\\_the\\_microstructural\\_variations\\_average\\_grain\\_size\\_on\\_UO\\_2\\_pellets\\_in\\_relation\\_to\\_the\\_Si\\_and\\_Al\\_contents\\_in\\_production\\_scale](https://www.researchgate.net/publication/237612197_Study_of_the_microstructural_variations_average_grain_size_on_UO_2_pellets_in_relation_to_the_Si_and_Al_contents_in_production_scale).
- Hastings, I.J. (1983). Effect of initial grain size on fission gas release from irradiated  $\text{UO}_2$  fuel. *Journal of the American Ceramic Society*, 66(9), c150–c151. <https://doi.org/10.1111/j.1151-2916.1983.tb10620.x>.
- Heyn, E. (1903). Short reports from the Metallurgical Laboratory of the Royal Mechanical and Testing Institute of Charlottenburg. *The Metallographist*, 5, 39–64.
- Higginson, R.L., & Sellars, C.M. (2003). *Worked Examples in Quantitative Metallography*. Maney.
- Koskenniska, S., Seppälä, O., & Kömi, J. (2020). A study on grain growth using a novel grain size calculation tool. *Procedia Manufacturing*, 50, 684–688. <https://doi.org/10.1016/j.promfg.2020.08.123>.
- Milena-Pérez, A., Bonales, L.J., Rodríguez-Villagra, N., Fernández, S., Baonza, V.G., & Cobos, J. (2021). Raman spectroscopy coupled to principal component analysis for studying  $\text{UO}_2$  nuclear fuels with different grain sizes due to the chromia addition. *Journal of Nuclear Materials*, 543, 152581. <https://doi.org/10.1016/j.jnucmat.2020.152581>.
- Song, K.W., Kim, K.S., Kim, Y.M., & Jung, Y.H. (2000). Sintering of mixed  $\text{UO}_2$  and  $\text{U}_3\text{O}_8$  powder compacts. *Journal of Nuclear Materials*, 277(2–3), 123–129. [https://doi.org/10.1016/S0022-3115\(99\)00212-3](https://doi.org/10.1016/S0022-3115(99)00212-3).
- Turnbull, J.A. (1974). The effect of grain size on the swelling and gas release properties of  $\text{UO}_2$  during irradiation. *Journal of Nuclear Materials*, 50(1), 62–68. [https://doi.org/10.1016/0022-3115\(74\)90061-0](https://doi.org/10.1016/0022-3115(74)90061-0).
- Une, K., Kashibe, S., & Ito, K. (1993). Fission gas behavior during post-irradiation annealing of large grained  $\text{UO}_2$  fuels irradiated to 23 GWd/t. *Journal of Nuclear Science and Technology*, 30(3), 221–231. <https://doi.org/10.1080/18811248.1993.9734473>.
- Vander Voort, G.F. (1993). Examination of some grain size measurement problems. In G.F. Vander Voort, F.J. Warmuth, S.M. Purdy, A. Szirmai (Eds.), *Metallography: Past, present, and future. 75th anniversary volume* (pp. 266–294). American Society for Testing and Materials.
- White, R.J. (1997). Equi-axed and columnar grain growth in  $\text{UO}_2$ . In *Water Reactor Fuel Element Modeling at High Burnup and its Experimental Support. Proceedings of a Technical Committee Meeting Held in Windermere, United Kingdom, 19–23 September 1994* (pp. 419–427). IAEA-TECDOC-957. International Atomic Energy Agency.
- Yang, J.H., Kim, K.S., Nam, I.H., Oh, J.S., Kim, D.J., Rhee, Y.W., & Kim, J.H. (2012). Effect of stepwise variation of oxygen potential during the isothermal sintering on the grain growth behavior in  $\text{Cr}_2\text{O}_3$  doped  $\text{UO}_2$  pellets. *Journal of Nuclear Materials*, 429(1–3), 25–33. <https://doi.org/10.1016/j.jnucmat.2012.05.034>.
- Zhong, Y., Gao, R., Li, B., Yang, Z., Huang, Q., Wang, Z., Duan, L., Liu, X., Chu, M., Zhang, P., Bail, B., Wang, Y., Cheng, L., Yan, B., Liu, T., & Li, R. (2021). Preparation and characterization of large grain  $\text{UO}_2$  for accident tolerant fuel. *Frontiers in Materials*, 8, 651074. <https://doi.org/10.3389/fmats.2021.651074>.

